AMRUPT Summer ‘18:

Russell Silva
Electrical and Computer Engineering, Cornell University
6/23/2018

Submitted to—
Dr. Julian Kapoor, Prof. Joe Skovira
Behavior/Electrical and Computer Engineering, Cornell University

I. Executive Summary

Animal Movement Research Using Phase-based Trilateration (AMRUPT) is a technology being designed for the localization of small animals in the field of ecology. This technology is proposed to suit ornithological studies involving individual- and species-level migratory patterns and social interactions. The system utilizes Phase Interferometry for use in estimating the angle of arrival (AoA) of radio signals. These systems have demonstrated resiliency in environments with high multipath interference and radio-frequency (RF) noise pollution, although performance scales strongly with the spatial scale of the receiver network. The design of AMRUPT will be forward compatible with phase difference of arrival ranging, a high precision localization approach developed for dense multipath indoor environments.

The embedded devices and RF modules chosen will keep our system low-cost while meeting hardware requirements for high spatial resolution. A low weight radio tag is being developed to transmit signals to radio base stations. These tags will transmit sub 1-GHz UHF frequencies. We will also be using inexpensive software defined radios (SDRs) for our basestations to obtain the radio-wave measurements required for AoA calculations. Each basestation will consist of a four RTL-SDR network and each RTL-SDR in the network will be connected to an antenna, an RF switch for synchronization purposes, and a Raspberry Pi. The Raspberry Pi serves as an embedded device which will collect and analyze the characteristics of the received radio signal. Each Raspberry Pi will have an open-source radio coding platform called GNU radio installed, equipped with the software protocols necessary for obtaining accurate AoA measurements, which will then allow us to triangulate a signal location.

II. Introduction

The accurate and real-time localization of small-bodied animals in the field of ecology is imperative to determine individual- and species-level migratory patterns, social interactions, and other key behaviors. Many attempts have been made to determine the positioning of animals temporally and spatially in the past, but have been either inaccurate (errors over five meters) or have required constant manual human intervention. Since direction finding requires wireless telecommunication, measurements have been thwarted by multipath interference from vegetation, electromagnetic interference, or other environmental conditions. Our objective is to develop a cost effective and automated system to track animal movements within the range of five meters while taking into account expected causes of error. Our proposed system consists of a receiver architecture that is built specifically for phase interferometry direction finding to facilitate accurate measurements from radio tags on tracked individuals.

III. Review of Literature

Many different techniques have been explored to achieve localization. Transmitted signals received at antenna array elements can be quantized at receivers to provide phase difference information such as in phase interferometry [4,6]. However, phase based measurements can be skewed by multipath effects in the environment by constructive and destructive interference [6]. In this literature review, we discuss methods to increase multipath resiliency in AoA methods and examine the strengths and weaknesses of widely used localization methods.

III. i. Received Signal Strength

One widely used method to position RF sources is Received Signal Strength (RSS). RSS can be used for localization through several different algorithms [5]; however, these metrics have been found to be unreliable. This is because RSS values fluctuate based on the complexity of the environment and are susceptible to interference from other transmitting sources [1], [15]. The complexity of the environment is a significant drawback in RSS because a signal received at an antenna will likely be a vectoral combination of time-delayed signals, causing RSS instability.

III. ii. Time Difference of Arrival

Another localization method is time difference of arrival (TDOA), in which the position of a transmitter is determined from the time differences between the arrivals of a signal at receiver stations in a network [1]. TDOA systems are not as susceptible to multipath effects because a line of sight (LOS) signal always arrives at receivers before reflected copies of the LOS signal. However, obtaining precise positioning from close proximity transmitters in TDOA is difficult because nanosecond synchronization among distributed ground-nodes is required to compare lightspeed propagated signals. The “Thrifty” system in [1] surmounts this drawback in TDOA systems by using direct sequence spread spectrum (DSSS) techniques in order to align a received signal with a local template code at a receiver based on a Psuedo Random Noise (PRN) code. Since PRN codes have low auto-correlation (correlation between the transmitted signal and local template is very low until peaks are perfectly aligned), their utilization in signal detection and alignment allows the arrival times of LOS signals to be determined accurately in time and aggregated on a centralized time frame for comparison among distributed ground nodes. Additionally, the use of DSSS techniques does not only aid with network synchronization but makes TDOA more robust against noise/interference by spreading the transmitted signal’s bandwidth. Modulation schemes employed for DSSS and the cross correlation capabilities of PRN codes are described in III. v.

It is important to note that the system developed in [1] was tested in a LOS environment, and was not built to be versatile in dense multipath environments. This is most likely due to the fact

that copies of a LOS signal can arrive at receivers with a delay greater than the chip length (binary 1's and 0's in the PRN sequence), adding chips in the LOS PRN code [18]. Perhaps this system can be further optimized against this problem by integrating RAKE receivers, which induces a time diversity on the transmitted signal so that independent multipath components separated by more than a chip time can be resolved [18].

III. iii. Angle of Arrival

A phase interferometry implementation that provides a good introduction to AoA calculation is a passive direction finding system in [4] developed for airborne signals. This system involves real time operation on multiple receivers driven by a common local oscillator (block diagram shown in Figure 1). Because this system was driven by a common local oscillator, the resulting intermediate frequency at each receiver could be compared without having to perform phase-offset synchronization. This system had an AoA accuracy with less than ± 2.5 degrees of error. Although the error rate is promising, this receiver system was designed to receive line of sight airborne signals. This does not account for the adverse effects of a cluttered environment where signals propagate near the ground, which will add additional factors to AoA error such as multipath interference.

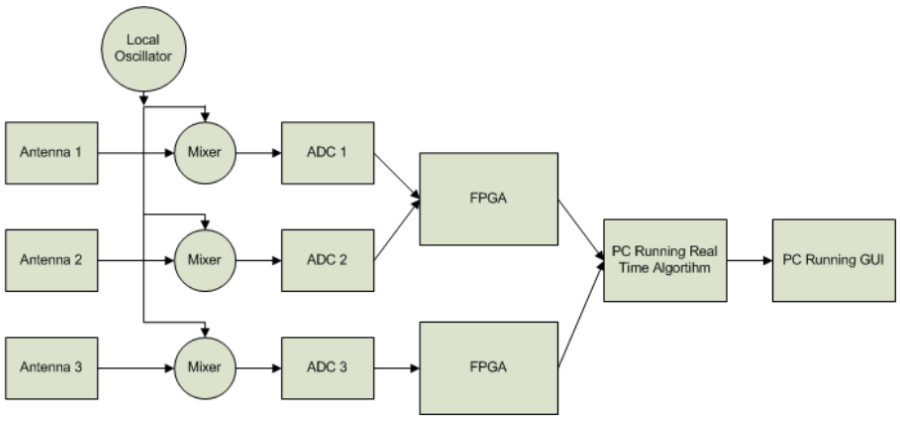

Figure 1: Block diagram for Phase Interferometry in Guerin, Jackson, and Kelly [4]

The direction of arrival (DOA) approach in [4], although refined through parameter simulations (i.e. the effect of antenna separation on AoA error), determines DOA solely based on the phase difference of antennas which could suffer from the effects of external noise (atmospheric, galactic, industrial) or system-inherent noise (antenna amplifiers, DF converts, A/D converters) [2]. The resolution of angle of arrival measurements in phase interferometry can be improved by using subspace techniques such as MUSIC and root MUSIC which are intended as a means of eliminating the effect of noise at an antenna array. In MUSIC and root MUSIC, a certain matrix notation is used to represent signals impinging on an antenna array which is entailed in Appendix

A. The MUSIC algorithm is described in Appendix B and the root MUSIC algorithm is described in Appendix C. In general, root MUSIC has a lower calibration error, sensitivity with respect to signal to noise ratio (SNR), and root mean square error (with respect to the estimated and measured DOA) than MUSIC [19]. Also, root MUSIC alleviates algorithm complexity. A drawback of root MUSIC is that it requires the use of uniform linear arrays [19]. Figure 2 displays the summarized steps of the MUSIC and root MUSIC algorithms.

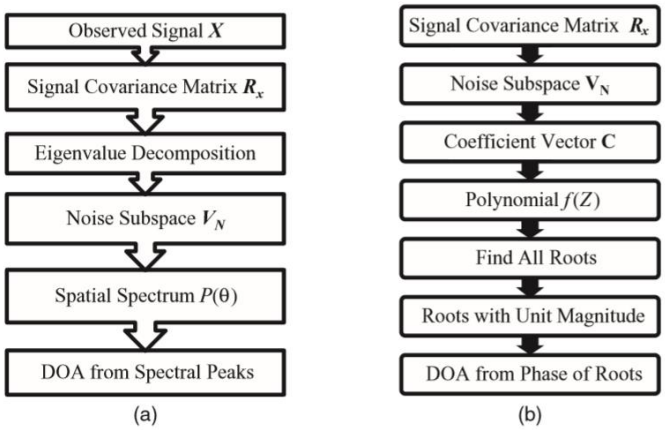

Figure 2: Block diagram of the (a) MUSIC and (b) root MUSIC algorithms [19]

Although accurate, MUSIC is a computationally expensive algorithm [14] and suffers from the effects of multipath interference [15]. [14] offers an alternative subspace technique, in which a modified switched beam system (SBS) is used. A SBS uses a fixed number of beams to scan the azimuthal plane. Even though SBSs such as Bartlett beamforming are computational inexpensive, they need low Signal to Noise ratios to work well, and they usually suffer low resolution as scanning the entire azimuthal plane will likely lead to multiple signal sources that are parallel to a steering vector. [14] proposes a novel cross-correlation based SBS (XSBS) technique which utilizes an omnidirectional signal beacon as a reference signal to compare signals within the angular range of interest. In this method, antenna weights (used in beamforming to scan the azimuthal plane) are all set to zero to receive the omnidirectional signal as stand alone antennas. Then, antennas are weighted according to the beamforming direction, and signals received at the weighted antenna array are cross correlated with the omnidirectional reference signal from the previous step. This method outperforms the MUSIC algorithm with more computational efficiency, but it is unclear how this method performs in a multipath environment.

In a multipath environment, the performance of MUSIC and root MUSIC degrades because refracted signals received at antennas will be correlated with the source signals themselves. This is a problem because separate signals in the signal subspace will be correlated, which goes against MUSIC's requirement for independent signal sources [8, 13]. A technique known as Spatial Smoothing can be used to remove the correlation of received signals by dividing the

antenna array into subarrays [8, 13]. If the number of antennas in the entire array is large enough, a noise subspace of uncorrelated vectors can be formed by averaging the correlation matrices of all subarrays and applying the averaged correlation matrix to the first step of MUSIC or root MUSIC. Nevertheless, spatial smoothing adds computational complexity and resolution scales with the number of antennas used. [13] proposes a new method, Covariance Differencing and Iterative Spatial Smoothing, to reduce the computation and antenna amount required by spatial smoothing. This technique subtracts an uncorrelated covariance matrix, corresponding to uncorrelated signals from resolved DoAs, from a covariance matrix computed with raw signals retrieved at an antenna array. This process is performed iteratively until no peaks appear in the MUSIC pseudospectrum, indicating an absence of correlated signals.

III. iv. Phase Difference of Arrival

The last localization method that will be investigated is phase difference of arrival (PDOA). Much like TDOA, PDOA systems compute a differential distance metric between a pair of receivers instead of an absolute propagation distances. The fundamental equation for obtaining a differential distance measurement in PDOA is $d = \frac{\varphi\lambda}{4\pi} + \frac{n\lambda}{2}$ where φ is the phase difference between two antennas, λ is the wavelength of the signal, and n is an ambiguous phase integer. Note that there is an extra factor of two integrated in the denominator of both terms. This is done to reflect that the RF wave travels double the tag to reader distance in a backscattering propagation.

To our current knowledge, only systems with radio frequency identification device (RFID) tags have implemented PDOA and most of these systems operate in indoor environments. RFID tags are highly desirable in PDOA systems, because the initial phase of the transmitted signal is known through conventional linear backscatter (a signal is transmitted to and reflected from a RFID tag) [15]. Moreover, the range over possible integers n in which a phase-integer disambiguation algorithm such as HMFCW [6, 12] would have to search for could be two orders of magnitude greater for outdoor environments with receivers spaced more than 100 meters apart. A solution to this drawback in outdoor PDOA systems is discussed in the Design Objectives section of this document.

To improve 3D localization in PDOA, Ma, Hui and Kan [6] proposes broadband harmonic backscatter and heuristic multi-frequency continuous wave (HMFCW) ranging. Broadband harmonic backscatter eliminates self-jamming in RFID readers by modulating the uplink response (tag to reader) on a second harmonic which is passively generated by non-linear devices inside the RFID tag. HMFCW ranging is used to resolve ambiguous phase cycle integers with maximum tolerance of multipath induced phase errors. [6] extends HMFCW ranging by using a genetic algorithm which selects an optimal frequency combination that maximizes phase error

tolerance. The larger the bandwidth of the multi-frequency transmission, the more robust the system will be to multi-path induced phase error.

Once the optimal frequencies are transmitted, and a phase integer n is determined reliably for each frequency, differential distances from a RFID tag to an antenna pair are computed and averaged for n_i and λ_i (in the fundamental PDOA equation) from indices 1 to K where K is the number of frequencies used for ranging. Ultimately, 3D positions are localized using optimized hyperboloid functions parameterized by differential distance measurements as shown in Figure 3.

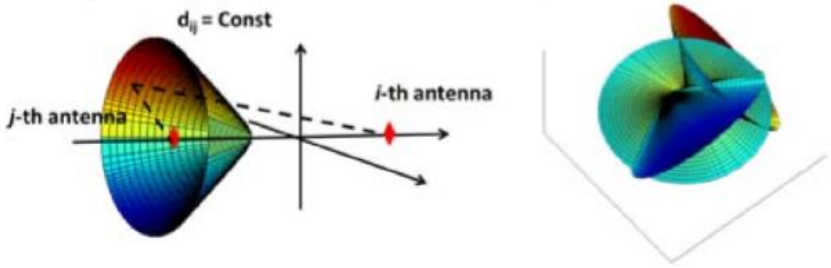

Figure 3: 3D localization by hyperboloid intersection [6]

This novel approach towards mitigating the effects of multipath interference, defined as the occurrence when radio waves reach a receiver via two or more paths, achieved localization with less than one-centimeter median error for 2D localization measurements.

A PDOA system with low-directivity receiving antennas in [12] uses AoA beamforming at antenna arrays to reject ranging measurements in transmission scenarios where multi-paths are stronger than LOS signals. The concept of coherence bandwidth is used, which classifies a range of frequencies which have a strong likelihood for amplitude and phase correlation. The coherence bandwidth is inversely proportional to the root-mean-square (RMS) multi-path delay spread of the transmission environment. For LOS signals stronger than multi-paths, two frequencies will be heavily correlated, independent of frequency separation. When Multi-paths are stronger than LOS signals, two frequencies will yield a large AoA gap when frequencies outside the coherence bandwidth are used. A graphic representation of this phenomenon is displayed in Figure 4.

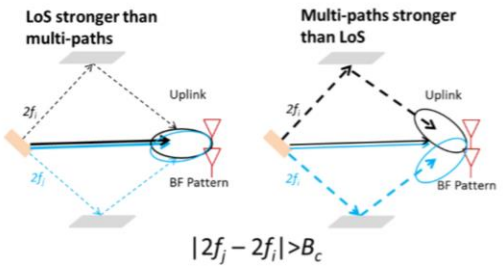

Figure 4: AoA Gap based on Strong LOS vs. Strong Multi-paths [12]

In [12], the maximum AoA gap is computed for frequencies within the HMFCW sequence. Every frequency pair spread further than the coherence bandwidth is considered for determining the maximum AoA gap. If the maximum AoA gap is above a certain threshold, the measurement is deemed unreliable and PDOA ranging is not performed. If this threshold is set large, measurements are more prone to be inaccurate. If this threshold is set small, reliable measurements may be rejected. [12] considers 30-40 degrees to be an optimal threshold.

III. v. Synchronization of Multi-channel Receivers and Distributed Ground Nodes

It is important to note that measurements used in calculating AoAs are obtained from antennas connected to the same receiver, instead of comparing parameters (e.g. TOA, phase) among disconnected receivers (TDOA/PDOA). In AoA systems with ADC's sharing a common clock signal; sampling does not start at the same time, resulting in bulk delays [9]. These synchronization errors can be corrected by cross correlating samples based on measured channel delays. These delays would be determined by monitoring signal dispersion among channels when a common signal (e.g. white noise) is delivered simultaneously to each ADC in a multichannel receiver.

In TDOA and PDOA, measurements must be compared among distributed ground nodes with no hard connection. Therefore, Sample-of-Arrival (SOA) values must be used instead of raw TOA or POA values for differential measurements to have an accurate common time base among receivers. A SOA value represents the index of the sample at which a local template code within a receiver lines up with the PRN code of the incoming signal [1]. In this way, the measurements of an incoming signal can be referenced to precise time values and compared with a common time base at a central basestation. The DSSS techniques examined mainly follow a two-step procedure: use a modulation scheme to inject a PRN code into a carrier wave before transmission, and then detect and cross correlate a PRN sequence at a receiver via a matched filter.

Before a radio tag transmits a DSSS signal, it injects a PRN sequence into a carrier signal (also known as a baseband signal) using a modulation scheme. One of these modulation schemes is On-off keying, in which the carrier wave is modulated on and off by taking the linear combination of a PRN sequence, consisting of pulses/square waves, and the carrier wave. Each pulse/square wave in the sequence is called a "chip". The smaller the chip duration, the larger the bandwidth of the modulated signal by the Heisenberg-Gabor uncertainty principle [17]. The modulation of a carrier wave with a PRN sequence increases the bandwidth of the transmission because the square wave itself is a collection of many different sine waves at varying frequencies. In a PRN code with an equal amount of one and zero code bits, half of the signal's

energy will be contained in the narrowband component and the other half in the unmodulated carrier component [1]. The transmitter used in [1] modulated the carrier wave for OOK by rapidly toggling the supply voltage of the power amplifier from a MCU digital output pin.

When an incoming PRN modulated signal reaches a receiver, a matched filter continuously runs a cross correlation operation, shifting the samples of the signal against a template at a specified sampling rate (i.e. four samples per chip) [19]. After each shift operation, the samples of the signal and template are multiplied and then accumulated to a total amount which indicates the level of signal/template alignment. A detection of a PRN signal is confirmed when this total amount exceeds a specified threshold.

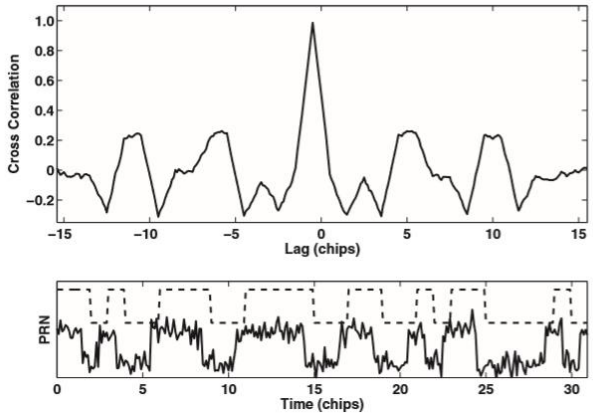

Figure 5: Time domain cross correlation of a PRN signal. [19]

The matched filter described above is extremely computationally expensive, because data streams of an incoming signal would have to be continuously cross correlated in the time domain to have prompt PRN detection and accurate SOA values. Since PRN codes can be represented as a complex spectrum of frequencies, the discrete fourier transform (DFT), at specified time intervals of the data stream (window size), can be compared against PRN time-shift sequences (i.e. 1, 1, 1, 0) for a time complexity of O(NlogN) instead of $O(N^2)$ [19]. The window size of the DFT is selected to be the minimum length necessary to contain the data from one complete tag transmission in order to further reduce the computational load (a shorter time domain window size in the DFT will also yield a finer frequency domain resolution).

III. vi. Low-cost Systems and Conclusion

In order to improve the cost effectiveness of direction finding, [1] has used low-cost RTL SDRs to extract in-phase and quadrature (I/Q) samples from incoming radio signals for TDOA and AoA calculations respectively. Direction Finding Implementations using RTL SDRs are promising alternatives to more expensive options by achieving up to 3.5m accuracy (under low multipath conditions) in TDOA [1] and by having an extensive hobbyist base with multiple Github repositories such as this one [10], demoed here. The advantages of having this repository

available to us is that it will provide us with a point of reference when implementing our code and hardware. This specific repository was a precursor to the RTL SDR system developed by Sam Whiting in [11].

The "Thrifty" system in [1] is promising, as ultra-wide bandwidth transmissions would be less susceptible to noise interference and signal refractions from a cluttered environment. However, this TDOA approach is limited by the effects of multipath interference, unless more complicated receiver hardware or software is used (i.e. RAKE receivers). The subspace smoothing methods for root MUSIC and MUSIC present powerful solutions to mitigate multipath interference. These AoA algorithms may be more suitable for close proximity (~100 meters) receivers outdoors than a TDOA system, which would be much more versatile with kilometer or greater receiver separations. A hybrid AoA/PDOA system with a combined coherent receiver and distributed ground node network could provide exceptional positioning for multi-frequency ranging within triangulated areas.

IV. Design Requirements

We have proposed the following objectives in the design:

1. The receiver system is low-power and can track up to 50 lightweight and low-power radio tags
2. System architecture is resilient in cluttered environment (unsusceptible to multipath interference, electromagnetic interference, and other environmental conditions)
3. System is able to achieve two dimensional high spatial accuracy (error for triangulation results is limited within 5 meters) with a 100-300m distance between receivers
4. Forward compatibility: Must be compatible with and adaptable to a multi-frequency PDOA approach for future versions.
5. System is cost-efficient (almost all components are commercially off-the-shelf)

The first objective is to successfully track the locations of 50 individuals in the testing environment. We need to design the tags as lightweight as possible since the individuals are small in size and heavy tags may affect the individuals' biological activities. To allow for the least human intervention possible during the tracking process, both the receivers and tags need to operate with minimal power consumption to increase automatic tracking period. In addition, both the transceivers (ground nodes) and tags (mobile nodes) follow a communication protocol in which the mobile nodes will go to sleep when they are not communicating with the ground nodes to reduce power consumption.

The communication protocol is an intended route for development, but has not yet been designed. It specifies that mobile nodes wake up every 5 minutes to prepare for data transmission to the ground nodes. The mobile node will receive a 5-second countdown signal once it wakes

up. As soon as the mobile node is verified to be within the receiver's range and has good link, it will be synchronized to global time before it is given a scheduled transmission time by the receiver or sent back to sleep again. If the mobile node is not within range of any receiver, it will go to sleep and wake up every 5 minutes to check whether it's within range again. The complexity of the ground-node to mobile-node communication protocol will be governed by how accurate our receivers are when taking angles of arrival measurements. If angles of arrival from at least three base stations intersect to a triangulation area of no more than 5 meter error (discussed further) over the specified tracking area, then tags will not have to be linked to different receivers depending on location and the same set of receivers can be used for all tags. The communication protocol will also be used for a multi-frequency system, which is a possibility in the future of this project.

Furthermore, the system must be able to obtain accurate results in a cluttered environment. We agreed that a real environment would have substantial multiple interference as there will be trees and rocks that can reflect a wireless signal. Multipath interference could result in multiple copies of a LOS signal with different DOAs. The effects of multipath interference and proposed solutions to the multipath problem are more amply discussed in the literature review section.

We agreed to set the tracking accuracy of our system to 5 meters because this is a minimum requirement to monitor the social interactions and movements of small mammal species. We propose a triangulation algorithm for Phase 1 of the project in order to acquire this accuracy: Phase 1 will be the development of the necessary base station algorithms and hardware setup to achieve an accurate angle of arrival measurement.

In the future, we plan to modify our system to better overcome the effects of multipath interference by frequency hopping to obtain minimum variation results (Phase 2). This modification will include AoA gap thresholding similar to the method used in [12]. Several frequencies spread evenly (with each frequency separation wider than the coherence bandwidth), between the lowest frequency and its second harmonic will be transmitted by the radio tag. The receiver will be coordinated with the radio tag to know when certain frequency values are transmitted, so that the receiving bandwidth can be adjusted accordingly. Using conventional Bartlett beamforming [7], an AoA gap for each consecutive frequency pair in the chosen sequence will be computed and compared. The in-phase and quadrature samples of the frequency which yields the lowest AoA gap will be further processed using root MUSIC (either one of the frequencies in the pair will be chosen). The number of frequencies used will be determined during testing.

If necessary, we plan to implement a multi-frequency PDOA system based on [6] that trilaterates positions of mobile nodes if a 5-meter accuracy level has not been achieved by previous efforts (Phase 3). Figure 6 illustrates error minimization with relation to AOA calculations:

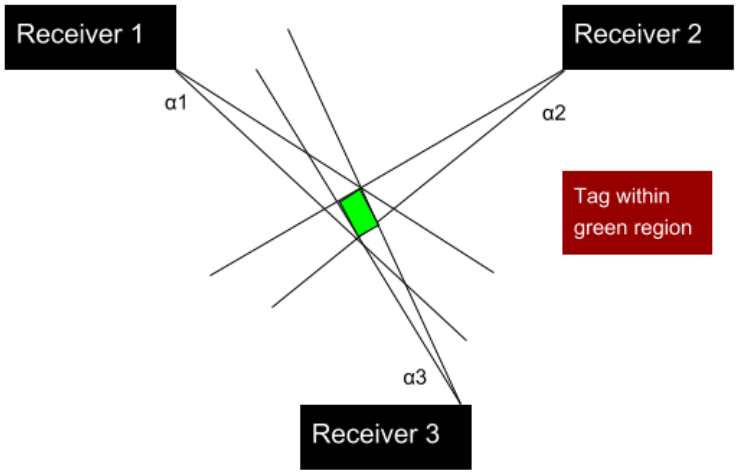

Figure 6: Error in triangulated area

In order to accomplish at least a 5 meter accuracy, a line of more than five meters cannot be drawn within the triangulated area of error. This area of error will be determined by α1, α2, and α3 (Figure 6) which resemble the angle of arrival error from receiver 1, 2, and 3 respectively. α1, α2, and α3 will be determined by phase difference errors from a transmitting RF signal to multiple antennas.

In order for the ground node network to track multiple tags continuously, we must have a system in mind to distinguish tags. Code-division multiple access (CDMA) is a very popular method for doing this due to the coding infrastructure. We plan to use a less complex time-division multiple access (TDMA) approach instead.

To address forward compatibility to the PDOA approach entailed in [6], the system must obtain reliable phase values at ground nodes in a distributed network. This will be accomplished by utilizing a radio tag that can modulate OOK signals, so that PRN codes can be used to obtain accurate SOA measurements at receivers. Once this is accomplished, the state of one RTL SDR within each coherent receiver will change back and forth from an antenna element used in MUSIC to a ground node that demodulates and collects phase SOA measurements. Receivers under this protocol will begin by triangulating an area for the radio tag, and then will proceed to hyperbolically determining a radio tag position using PDOA. This is done to reduce the parameter space over which the phase-integer disambiguation algorithm would need to search (e.g. AoA triangulation might produce a 10-meter area of high confidence for the location of a transmission, and the phase-based DOA ranging algorithm could then search within this area to further refine position estimates).

V. Technical Approach

The entirety of the proposed direction finding system consists of radio transmitters and receivers. This section will focus primarily on receiver design as the lightweight radio tags have already been developed.

V. i. Receiver Architecture

We first propose a receiver architecture that consists of RTL SDRs to simplify wireless communication and improve the cost effectiveness of this project. The receiver architecture is outlined in Figure 7. Note that this includes 4 antennas connected to four individual RTL SDRs, so that a linear array of substantial size can be used in AoA subspace methods.

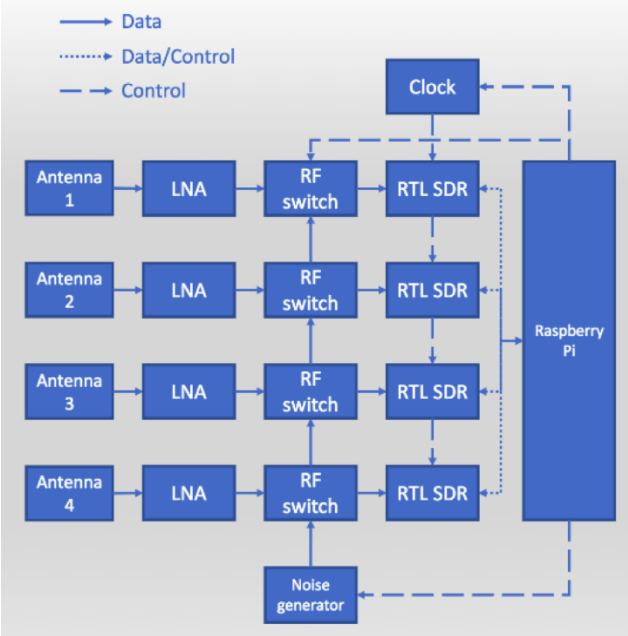

Figure 7: Receiver Architecture

Before choosing the RTL SDR and Raspberry Pi for the above architecture, we considered the following ideal specifications for a software defined radio and embedded device:

1. A sub 1-GHz device for VHF or UHF frequencies transmitted from radio tags. We choose a lower frequency band (relative to most RF applications) to mitigate multipath interference and better determine the phase difference of signals. Previous systems have used ~150 MHz as the operating frequency of transmitters because of the impact of large trees on multipath interference.

2. A very high sample frequency during the analog to digital conversion of RF signals. This is essential for mitigating adverse effect from noise when determining accurate phase differences from radio waves moving at the speed of light. However, a sampling frequency above twice the radio frequency (constant in a non-frequency modulated signals) is not needed. Sampling rates are further discussed in section IV. Vii. “RF Wave Reconstruction and Matlab Simulation”.
3. Ample UART/I2C/SPI/GPIO connections for data logging and transfer
4. Contains every component necessary for receiving an RF signal from an external antenna – ADC, local oscillator, etc.
5. Extremely high RF sensitivity and blocking performance
6. Programmable and highly used by the public – helpful for finding more tutorials and readily available information on the device
7. Low power and low cost

From this list of specifications, the RTL SDR was chosen. An RTL SDR is a low-cost software defined radio which uses quadrature demodulation and receives frequencies from 500 kHz to 1.75 GHz. The RTL SDR has a maximum sample rate of 2.4 MS/s. At this sample rate, the RTL SDR not drop any samples from data extraction. The RTL SDR uses a USB interface which can be connected directly with the Raspberry Pi. The receiving frequency and bandwidth of the RTL SDR can be dynamically adjusted from a terminal or software running on the Raspberry Pi.

Instead of having to manually hook up separate components together for the proposed receiver architecture, we will order units from a company focused on multichannel RTL SDR integration called “coherent-receiver.com.” This company provides a 4-channel RTL SDR basestation with external components to coherently receive RF signals from radio tag sources. These external components include antenna switches and an integrated clock card. Figure 8 displays this device. The clock card is used to send a common clock signal to all four RTL SDRs. The common clock signal is a 28.8 GHz signal used to synchronize samples received at each RTL SDR. Even in systems with ADC’s sharing a common clock signal, sampling does not typically start at the same time (bulk delays) [9]. Therefore, a noise generator (which can be replaced by an external function generator) is utilized during noise switching. In the noise switching process, antenna switches synchronously transition from a common noise signal to individual antenna signals. This antenna switching can allow a cross correlation function to solve bulk delays by aligning channels based on the delays experienced between channels when the noise generator is on.

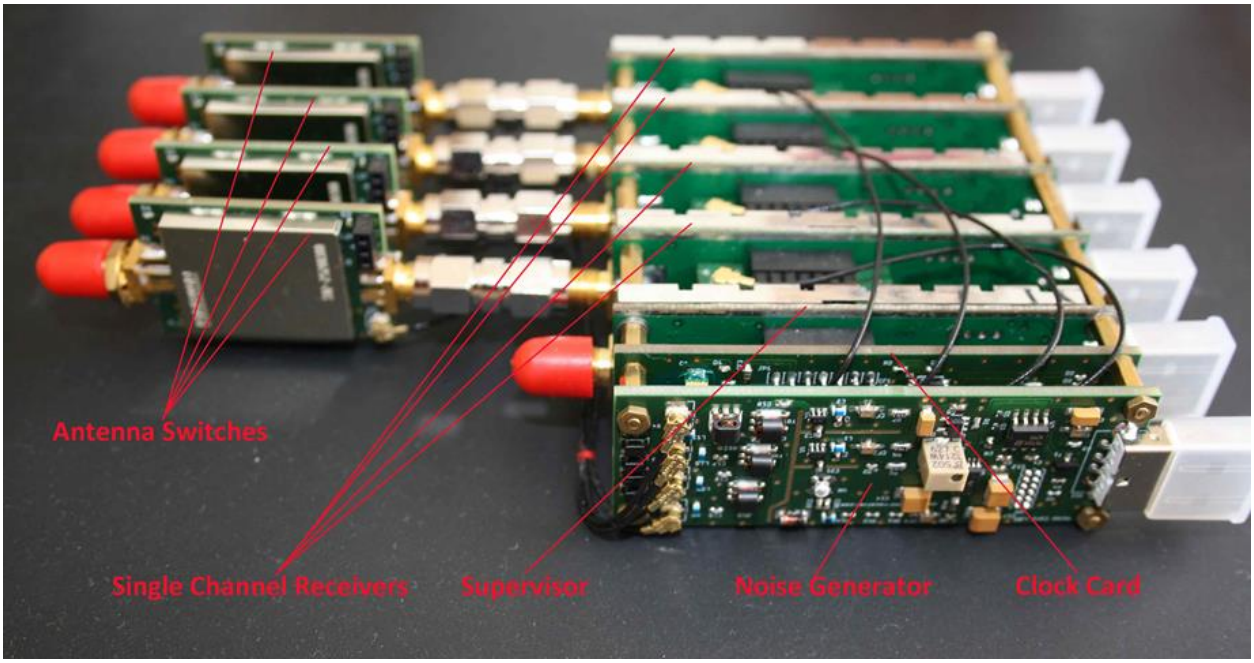

Figure 8. Coherent Receiver Components

In addition to the coherent receiver, low loss male to female SMA Connector wires are proposed to separate whip antennas connected to the RTL SDRs on the coherent receivers. The lengths of the connectors' insulated wires will accommodate distances around half the wavelength of the incoming VHF RF signal (anywhere from 0.5 to 2.5 meters for VHF signals). In other words, the SMA connector wires will have lengths that are long enough so that antennas can be separated at half the wavelength of the incoming RF signals.

Each RTL SDR will have a USB connection intended for an individual port on a Raspberry Pi. The Raspberry Pi serves as an embedded device which collects data samples from each RTL SDR. We intend to develop all of our receiver software on the Raspbian operating system (OS).

V.ii. Software Overview

The proposed software consists of sampling received RF signals at the RTL SDRs in the coherent receiver and performing digital signal processing (DSP) methods on these samples to generate accurate AoA measurements. All of the DSP will be implemented in c/python within a standard raspbian operating system.

In last semester's system, we used a MUSIC implementation that was completely encapsulated into a GNU Radio Custom Block developed by Ettus Research. Ettus Research is a National Instruments company that is the world's leading supplier of software defined radio and publishes software that can be used with its products online. We choose to use custom blocks developed by Ettus Research because they are very well documented and have been empirically tested (see

[16]). One of the major procedures of this summer's work will be developing our own version of root MUSIC/autocorrelation using the ETTUS modules as a basepoint for the software implementation outlined in Figure 9.

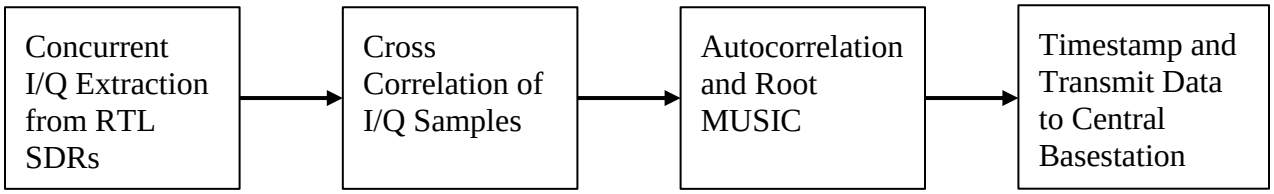

Figure 9: General software procedure for the proposed system, starting from the extraction of I/Q samples to AoA calculation and transmission.

The autocorrelation step of this procedure computes a covariance matrix using subspace smoothing. This covariance matrix is inputted into the root MUSIC algorithm (Appendix C). I/Q extraction, cross correlation, and internetwork transmission are outlined in sections V. iii., V. v., and V. vi. respectively.

V.iii. Sampling from the RTL SDR

Since RTL-SDRs use a quadrature demodulator, radio signals are sampled into in-phase and quadrature values corresponding to the real and imaginary components of an incoming RF signal. Parallel I/Q extraction from multiple RTL SDR receivers can be retrieved by writing to files from the Raspbian terminal using the following code once RTL SDR drivers are setup correctly (a driver setup tutorial can be found in steps 0-2 in this link):

```
rtl_sdr -d0 -f 1125000000 -g 35 -s 2500000 -n 50000000 -N FMcapture0-2.dat &
rtl_sdr -d1 -f 1125000000 -g 35 -s 2500000 -n 50000000 -N FMcapture1-2.dat &
rtl_sdr -d2 -f 1125000000 -g 35 -s 2500000 -n 50000000 -N FMcapture2-2.dat &
rtl_sdr -d2 -f 1125000000 -g 35 -s 2500000 -n 50000000 -N FMcapture2-2.dat &
```

Where -d specifies a RTL SDR channel, -f specifies frequency, -g specifies RF gain, -s specifies sampling rate (which equates to bandwidth), -n specifies number of samples, and -N specifies a file name. [20]

V. iv. Asynchronous Execution

We will have to design our program to run smoothly without any data overflows or AoA time lag. Since the data samples will be processed into separate files, the number of samples for each file will have to be chosen carefully for future steps in the software procedure. The most significant steps for choosing sampling sizes include:

1. Cross Correlation Length and Rate: Given the potential uncertainty in sample conversion start time, a substantial length of data will have to be inputted to the cross correlation function [9]. 262,144 samples would be a good place to start. Since this long cross correlation is expensive, the cross correlation function will be called at a set rate (every 10 iterations – every 2,621,440 samples). For this reason, the main script will create data files with 262,144 samples dedicated to cross correlation. Also, the main script will make sure the receiver channels are switched to the noise source before the 262,144 samples are collected. This is to ensure that the alignment of channels will be based on a reference signal, and not on a signal transmission.

   After the cross correlation function computes a delay for the three signals ahead in time, the main script will switch the receiver channels back to the antenna state. Then, the main script will create data files of the following sample length: 2,621,440 – 262,144 + longest delay sample length. The longest delay sample length (corresponding to the signal most ahead in time) is added so that no channel runs out of samples after applying delays. Figure 10 may help visualize this.

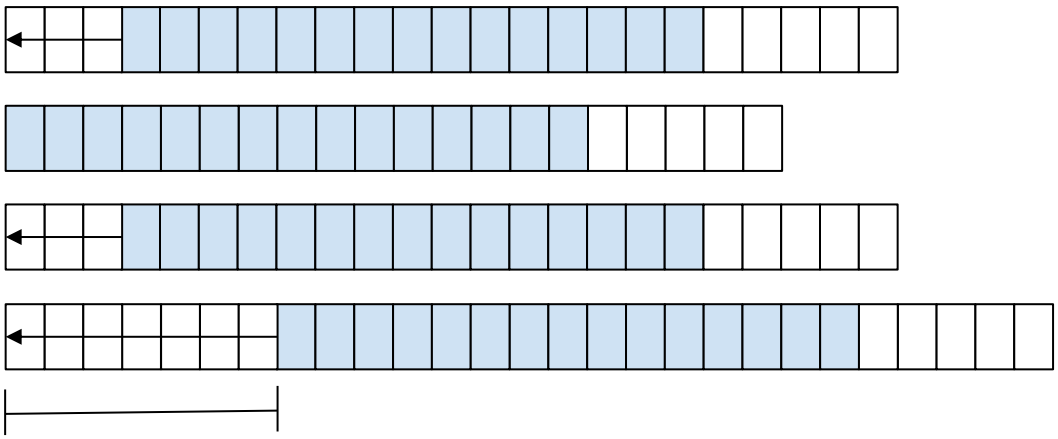

Figure 10: The longest delay sample length is added to the data extraction length so that no channel runs out of samples for future processing once samples are aligned. The blue squares represent the number of samples that will be used for future computation (white squares discarded). The number of samples that will be available for future computation will be 2,352,256 (2,621,440 – 262,144).

2. Autocorrelation Snapshot Size: The number of samples inputted into the autocorrelation (and consequently the MUSIC algorithm) is denoted by snapshot size. A sufficiently large snapshot size is recommended in [16] to achieve a reasonable amount of spatial averaging effect when computing the sample autocorrelation matrix. This reduces the RMSE in DoA estimation. The default value for snapshot length is 1024 which achieved a 12.5 MS/s sample rate per stream in a benchmark test for generating AoA values [16]. Since 2,352,256 samples

will be remaining after cross correlation, AoA values can be computed 2297 times (2,352,256 / 1024) and averaged under this snapshot length. To reduce computational complexity, most of the samples from the cross correlation will be discarded, so that the autocorrelation function can be rate-limited.

In summary a cross correlation function will be called with a set number of samples. The proceeding data extraction will have an increased number of samples + the longest delay sample length. Using the result of the cross correlation function, data streams from separate channels will be aligned to fix bulk delays. The resulting data streams will then be rate limited into the autocorrelation function. Because of the asynchronous nature of this procedure, data extraction and functional procedures cannot happen at the same time. However, there will be no compounding lag time because data files will be cleared before each computation, so that the next data extraction will be in real time. In other words, each computation will take an arbitrary amount of time which does not compound to an overall delay because the data input channels will be reset at each computation.

V.v. Cross Correlation of I/Q Samples for Multiple Channels

In order to solve bulk delays between the RTL SDR datastreams, a protocol will be developed similar to the one encapsulated in the GNU Radio sample offset block from [9]. This sample offset program only computes a cross correlation between two signals, so the cross correlation functionality in this program will have to be modified for four separate signals in our system.

The code within the sample offset program computes the delay of one signal over another by taking a Fast Fourier transform of both signals, convoluting both signals in the frequency domain, and then taking the inverse Fast Fourier transform of the convolution to find the maximum argument (time value) of the output signal's amplitude in the time domain. The median of the peak values (from the Fast Fourier transform convolution) corresponds to the delay between the two signals.

Once offsets between the signal channels have been determined, the program will return the delay values and channel numbers corresponding to the three signals ahead in time.

V. vi. Raspberry Pi Datalogging and Triangulation

Once we obtain reliable AOA data from each raspberry pi basestation, we will append code to the root MUSIC program to store timestamped AoA measurements into a text file. The information in this text file will be transmitted to a central basestation for triangulation in either two ways:

1. Attaching a wireless mobile broadband modem to the Raspberry Pi similar to the procedure used in [1]. This procedure is relatively easy to implement and is cost effective; however, it comes with the cost of several drawbacks. The system clocks of several Raspberry Pi devices can differ up to 0.5 seconds which is detrimental to detection matching. This issue can be solved by using a dedicated beacon transmitter to pair detections with unique events, which can rectify timestamp offsets of up to 30 s [1]. The use of a usb broadband modem will also require mounting an external board to the Raspberry Pi with extra usb connections (the four usb ports on the Pi will be consumed with RTL SDR connections) and an internet connection, which may be unavailable in several wildlife tracking areas.

2. Connect long range RF modules (i.e. CC1310) to each Raspberry Pi ground node and a central basestation through an I2C or SPI connection. These modules would transmit the data with frequencies that do not interfere with the radio frequencies used in localizing the radio tags. The major drawback of this method is that transmissions to the central basestation would have to be coordinated so that multiple receivers do not transmit data to the central basestation at the same time. Also, data might be lost if environmental conditions prevent these transmissions from reaching the central basestation.

Once AoA measurements from separate basestations are reliably transmitted to the central basestation, triangulation will be performed using these measurements according to the pseudocode below:

```
class Coordinate:
    def _init_(self, x = 0.0, y = 0.0):
        self.x = x
        self.y = y

    #Finds intersection of two lines (y = mx + b)
    def intersect (m1, b1, m2, b2):
        intersection = Coordinate()
        xval = float(b2 - b1) / float(m1 - m2)
        yval = xval * m1 + b1
        intersection.x = xval
        intersection.y = yval
        return intersection

    #Finds the centroid of the triangulated area
    def centroid(vertex1, vertex2, vertex3):
        center = Coordinate()
        center.x = (vertex1.x + vertex2.x + vertex3.x) / 3.0
        center.y = (vertex1.y + vertex2.y + vertex3.y) / 3.0
        return center

    #Parameters are decimal angle of arrivals calculated at
    #each base station and coordinate positions of each
```

```
#base station.
def triangulated area(aoa1, aoa2, aoa3, receiver1, receiver2, receiver3):
    #Converts angle degrees to slope
    slope1 = math.tan(aoa1)
    slope2 = math.tan(aoa2)
    slope3 = math.tan(aoa3)

    b1 = receiver1.y - receiver1.x * slope1 #y = mx + b
    b2 = receiver2.y - receiver2.x * slope2
    b3 = receiver3.y - receiver3.x * slope3

    intersection1 = intersect(slope1, b1, slope2, b2)
    intersection2 = intersect(slope2, b2, slope3, b3)
    intersection3 = intersect(slope1, b1, slope3, b3)

    position = centroid(intersection1, intersection2, intersection3)
    return position
```

At the central basestation, a separate program will build a primary text file for the triangulation measurements computed. The program will also create a time and tag label for each measurement on file. In a future iteration of this system, a tag label will be determined by the approximate time the measurement was made (by referring to the TDMA schedule). There will be a real time clock onboard to monitor the time and help create the time and tag label for each measurement.

V. vii. Frequency Hopping and Network Communication

This section overviews the implementation for the Phase 2 system modification mentioned in the Design Objectives section. A frequency hopping protocol will be encoded into the central basestation that will send mobile and ground nodes a list of frequencies and the specific times those frequencies will be transmitted. In this way, the receiving frequency and bandwidth at RTL SDRs can be adjusted according to the frequency sent by a radio tag at a specific time. This central basestation to network communication will also provide a starting point for the TDMA communication protocol to be implemented in a future iteration of this system.

Another Phase 2 modification of our system entails using an AoA gap thresholding technique similar to the method used in [12]. After the cross correlation step of the software flowchart displayed in Figure 9, data streams will be inputted into a conventional Bartlett beamforming algorithm and stored into a data stream file for possible future use. Using conventional Bartlett beamforming, an AoA gap for each consecutive frequency pair in the frequency hopping protocol will be computed and compared. The frequency that yields the lowest AoA gap will determine what samples (in the data stream file) should be used in the root MUSIC algorithm. The resulting AoA measurements from the root MUSIC algorithm will be transmitted to the central basestation as described in the previous section.

VI. Management Plan (W: Week)

Tasks(Below)	W1	W2	W3	W4	W5	W6	W7	W8
Phase 1								
Hardware Configuration and Checking								
1. Clock Card I2C Integration								
2. Noise Source Input and monitoring RF Switching between noise and SDR sources								
Software Setup								
1. Cross Correlation C/C++ Code								
2. Asynchronous Execution Setup								
3. Autocorrelation Code								
4. root Music Code								
5. AoA Datalogging								
6. Central Basestation Configuration and Triangulation								
Testing and Deliverables								
1. Angle of Arrival Measurement Testing Protocol (as entailed in the Deliverables Section)								
Phase 2								
1. Central Basestation communication to CC1310 transmitters for frequency hopping								
2. AoA Gap Minimization Code on receiver basestations								
Append design implementation and empirical testing sections to this paper and GitHub Documentation								

The above plan for AMRUPT allocates a set of tasks/responsibilities corresponding to eight weeks of the summer to work on this project, which are as follows:
Week 1: 6/24/2018 – 6/30/2018
Week 2: 7/1/2018 – 7/7/2018
Week 3: 7/8/2018 – 7/14/2018
Week 4: 7/15/2018 – 7/21/2018
Week 5: 7/22/2018 – 7/28/2018
Week 6: 7/29/2018 – 8/4/2018
Week 7: 8/5/2018 – 8/11/2018
Week 8: 8/12/2018 – 8/18/2018
Note: AoA testing is performed at the end of Phase 1 and Phase 2.

VII. Deliverables

At the end of the summer, we plan to achieve at least a 2.8 degree angle of arrival accuracy to obtain sub 5 meter triangulation accuracy (s =$r\theta$, 5 = (100)(~2.8 $*$ $\frac{\pi}{180}$)) for a radio tag within our minimum range objective of 100 meters.

Our test strategy is to first test the prototype from an ideal and small environment to avoid complications with a large environment. Our first tests will consist of setting the tag 20 meters away from one coherent receiver. These tests will be performed in a small open area with no large natural vegetation to avoid the effects of dense multipath interference. If all goes well with the first tests, the proceeding experiments will be performed in such a way that when we move the tag, AOAs will be updated along the way. As a comparison, we will also measure the expected angle by a protractor. The appropriate errors and standard deviations for these data trials will be computed. The next experiment will be to test the positioning of a tag in an environment with multipath interference. Some large blocking items such as large desks or chairs could be put in the same testing environment to see how our system handles multipath interference. Again, many trials of measured and expected AOAs will be tested and compared in the block-free and with-block environments. We will repeat these test suites with 50 and 100-meter detection ranges. Again, we will start with the block-free environment, collecting data for both the measured and expected AOAs, and then move to the with-block environment. Additionally, we will perform additional tests in outdoor woodland areas, as this system is being developed for this type of environment.

Another important aspect of testing is to verify the speed of the signal processing and if the data logging is fast enough for tags attached to small birds that move relatively fast in the environment. Therefore, it is helpful to develop a performance test to measure the runtime of the signal processing programs. During the performance test, a tag will be put on a human, who will move at a relatively fast pace to simulate a fast-moving animal in the environment. The movement of the tag will be pre-determined, so we know in advance what AOA values are expected. The calculated AOAs from the program will be compared against the expected values and the percentage error will be calculated.

During summer testing, a narrowband continuous wave will be sent from a CC1310 acting as a radio tag. The polarization of the PCB antenna on the CC1310 is unclear, so a JSC to SMA connection may have to be made to an external whip antenna because the receivers use linearly polarized whip antennas. It is beneficial for an RF system to have equal polarization for receivers and transmitters to avoid propagation losses [2].

There will be individual weekly updates starting from the week of June 24th. The weekly updates will include sections on problems, goals, general approach, solutions/testing strategy,

and planned course of action with any references used to solve the problem. At the end of the summer, design implementation and empirical testing sections will be appended to this paper. There will also be all-encompassing documentation on the work performed this summer.

VIII. Conclusion

In order to accomplish the localization of small animals, we plan to develop a cost effective and automated system to track animal movements within the range of five meters while taking into account expected causes of error. Our proposed system consists of a receiver architecture that is built specifically for phase interferometry direction finding to facilitate accurate measurements from radio tags on tracked individuals. In order to accomplish this, a low weight radio tag is being developed to transmit signals to radio base stations. These tags will transmit sub 1-GHz UHF frequencies.

Appendix A. Matrix Notation for Received Signals at Antenna Array Elements [3, 7, 8]:

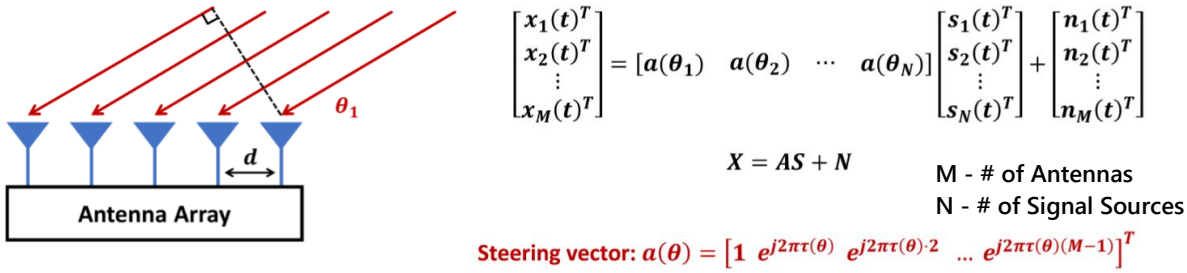

Figure 11: Antenna Array Matrix Representation [7]

Each element in the array is spaced equally at distance d from each other with d less than or equal to half of the wavelength λ of the incoming signal. $\lambda/2$ spacing is applied to avoid phase ambiguity (a phase difference at antennas spaced greater than $\lambda/2$ can be +/- πn where n is the number of ambiguities).

As shown in the diagram, there is a radio wave which impinges upon each antenna array element with angle θ_1 . The received signal(s) at each antenna can be represented by a matrix "X" formed of vectors $x_M(t)$where the prefix M denotes the antenna number. The phase shift at each antenna of an incoming signal can be put into a MxN matrix "A" formed of steering vectors (the number of steering vectors correspond to the number of signal sources). A steering vector can be used to represent the phase shift per antenna of an incoming signal, with τ_θ = dcosθ / λ terms derived from the extra distances a radio wave must travel to antennas based on the received angle of the signal. The τ_θ term in each array element in the steering vector is multiplied by the array element's index in the exponent of the phasor. This is because the second array element has 1x

the phase shift, the third array element has 2x the phase shift, and so on. Signals denoted by $s_N(t)$ are represented in phasor notation as $s_N(t) = Ae^{j\omega t}$ where the prefix N denotes a signal number (there can be multiple incoming signals), A represents an amplitude, and ω represents the frequency of the signal. $n_M(t)$ terms are noise vectors which represent external or system-inherent effects on signals transferred into a digital signal processor.

Appendix B. Multiple Emitter Location and Signal Parameter Estimation [3, 7, 8]:

Using the assumption that incident signals and noise vectors are uncorrelated, we can take the covariance "Rxx" of the X = AS + N matrix formulation from Appendix A and set it equal to $ARssA^H + \sigma^2 I$ where the superscript H denotes the Hermitian transpose of a matrix. Rss is an NxN matrix with rank equal to N if the source signals are independent. An important consideration here is if the signals are correlated, the signal subspace will have dependence, which disrupts the performance of the MUSIC algorithm. This often occurs under multipath interference in which refracted signals can be correlated with source signals. Methods such as subspace smoothing or iterative methods described in [13] can improve the resiliency of MUSIC under multipath conditions.

Following the $ARssA^H + \sigma^2 I$ from before, A is a matrix composed of the steering vectors of the incoming signals impinging on the antenna array. It will have as many positive eigenvalues as signal sources (N) because each signal source will contribute an independent eigenvector in the signal subspace. The rest of the eigenvalues (M – N eigenvalues left) will correspond to eigenvectors in the noise subspace. The crucial step of MUSIC is partitioning the eigenvectors of positive eigenvalues into a signal subspace and the eigenvectors of zero eigenvalues into a noise subspace. Once a noise subspace is found, the Hermitian transpose of the subspace is multiplied to a calculated steering vector (based on the positions of antennas in the array) for a range of all possible angles. This calculation will result in zero values for situations in which the noise subspace is orthogonal to the steering vector (representative of the signal subspace), which will occur precisely when the AoA of a signal source is aligned with the AoA of the chosen steering vector.

Step by step, the algorithm is as follows:
1.Calculate the covariance matrix of the vector of complex signals, the number of source signals must be known beforehand.
2. Perform an eigenvalue decomposition of the covariance matrix.
3. Sort the eigenvectors according to their eigenvalues in greatest to least order.
4. Place the last M - N eigenvectors into a noise subspace matrix Q
5. Compute steering vector $a(\theta)$for all angles within [0, 180] based on antenna spacings and signal wavelength. (Can reduce computationally complexity here by focusing on a smaller angle range in a combined TDOA/PDOA approach).

6. Plot the pseudospectrum $p(\theta)=\frac{1}{a^H(\theta)QQ^Ha(\theta)}$, where the resulting plot has an x-axis in degrees and a y-axis in decibels. The peaks of the graph correspond to angle of arrivals of source signals.

A comparison of music against conventional beamforming, maximum likelihood, and maximum entropy methods is shown in Figure 12.

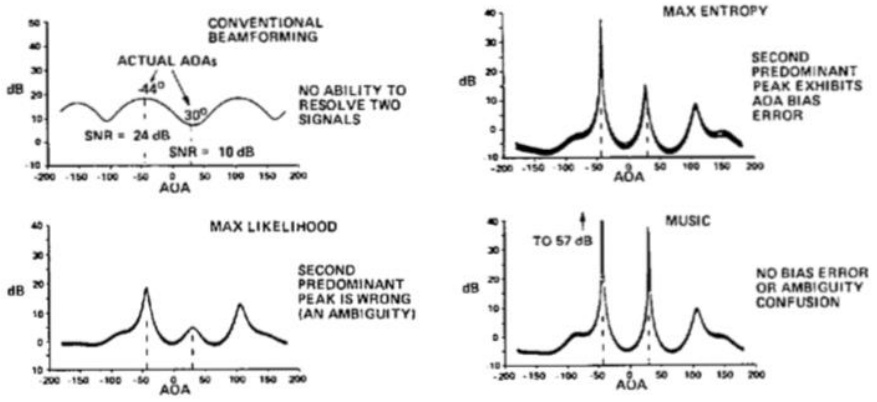

Figure 12: Azimuth-only performance in common AoA methods [3]

Appendix C. Root Multiple Emitter Location and Signal Parameter Estimation [16, 21]:

Recall from Appendix B that the denominator of the pseudospectrum was $a^H(\theta)QQ^Ha(\theta)$, where $a(\theta)$ is the steering vector (computed for an arbitrary number of angles within a direction finding range) and Q is the noise subspace retrieved from an eigenvalue decomposition of the covariance matrix. Also, recall the form of the steering vector from Appendix A, where each element of the vector represents a phase shift at an antenna index. The denominator of the pseudospectrum can be expressed as in [16] where a is v and Q is Un:

$$
\begin{aligned}
Q(z) &= \mathbf{v}^T(1/z)\mathbf{U_N}\mathbf{U_N^H}\mathbf{v}(z) \\
&\overset{(a)}{=} \sum_{m=0}^{N-1}\sum_{n=0}^{N-1} z^{-m}\,\mathbf{U}_{\mathbf{N}}^2(m,n)\,z^n \\
&\overset{(b)}{=} \sum_{-N+1}^{N-1} u_l\, z^l.
\end{aligned}
$$

In b), u_l corresponds to the sum of elements under the noise subspace matrix's diagonal for $l < 0$ and the sum of elements over the noise subspace matrix's diagonal for $l > 0$. l can take on any value between N – 1 and N + 1 where N corresponds to the number of antennas. Just imagine for now that N – 1 and N + 1 is M – 1 and M + 1 to avoid confusion with the explanations in Appendices A and B (where M is the number of antennas and N is the number of signal sources).

By multiplying each noise subspace sum with each element in the steering vector, and adding all of these results up, a polynomial of size M – 1 will result. From this polynomial, there should be N roots that lie on the unit circle which will correspond to the AoAs of incoming signal sources. The reason for there being N roots on the unit circle ties into the orthogonality of noise and signal subspaces. This orthogonality means that a multiplication of a computed steering vector (for an angle of arrival of an incoming source signal, representing a vector from the signal subspace) and the noise subspace should result in a very tiny value if not zero. Furthermore, the roots of a polynomial are values that cause the polynomial to evaluate to zero.

Due to the presence of noise, the roots may not necessarily be directly on the unit circle. For this reason, the N (number of signal sources) closest roots to the unit circle are chosen to represent the angles of incoming source signals. Determining the closest roots to the unit circle can be done by taking the Euclidean distance of each root (for a real and complex value). The roots with Euclidean distances closest to 1 will be chosen.

Once the roots are determined, the AoA for each incoming signal is determined by the following expression:

$$\theta_n = arcsin(\frac{\lambda}{2\pi d} arg(z_d))$$

Where z_d corresponds to an individual root out of N roots, λ is the wavelength of the signal, and d is the antenna separation. The function arg refers to $tan^{-1}(\frac{y}{x})$ from the complex form $x + iy$.

Appendix D. Works Cited

[1] Krüger, S W. “An Inexpensive Hyperbolic Positioning System for Tracking Wildlife Using off-the-Shelf Hardware.” May 2017.

[2] Rohde & Schwarz “Introduction into Theory of Direction Finding,” Radiomonitoring & Radiolocation, Catalog 2011/2012.

[3] Schmidt, R. “Multiple Emitter Location and Signal Parameter Estimation.” *IEEE Transactions on Antennas and Propagation*, vol. 34, no. 3, 1986, pp. 276–280.

[4] D. Guerin, S. Jackson, and J. Kelly, “Passive Direction Finding: A Phase Interferometry Direction Finding System for an Airborne Platform,” Oct. 10, 2012. https://web.wpi.edu/Pubs/E-project/Available/E-project-101012-211424/unrestricted/DirectionFindingPaper.pdf.

[5] D. Zhang, J. Ma, Q. Chen and L. M. Ni, "An RF-Based System for Tracking Transceiver-Free Objects," Fifth Annual IEEE International Conference on Pervasive Computing and Communications (PerCom'07), White Plains, NY, 2007, pp. 135-144.

[6] Y. Ma, X. Hui, and E. Kan, “3D Real-time Indoor Localization via Broadband Nonlinear Backscatter in Passive Devices with Centimeter Precision,” Oct. 3, 2016. https://dl.acm.org/citation.cfm?id=2973754.

[7] Wenguang Mao “Approaches for Angle of Arrival Estimation” https://pdfs.semanticscholar.org/presentation/723e/3f7ce640f425671d4e0af7d23b82e04a402e.pd
[8] Fan, H. Howard “Direction of Arrival Estimation (DOA) in Interference & Multipath Propagation,” GIRD Systems, Inc.
[9] Whiting, Sam, et al. “Time and Frequency Corrections in a Distributed Network Using GNURadio.” 2017.
[10]“Tejeez/rtl_coherent.” GitHub, 6 July 2016, github.com/tejeez/rtl_coherent
[11] Whiting, Sam, et al. “Time and Frequency Corrections in a Distributed Network Using GNURadio.” 2017
[12] Y. Ma, X. Hui, P. Sharma, E. Kan. “Indoor Passive Device Ranging by Low-directivity Antennas with Centimeter Precision.”
[13] E. M. Al-Ardi, R. M. Shubair, and M. E. Al-Mualla. “Direction of Arrival Estimation in a Multipath Environment: an Overview and a New Contribution,” Aces Journal, Vol. 21, No.3, November 2006.
[14] Badawy, Ahmed, et al. “A Simple Angle of Arrival Estimation System.” *2017 IEEE Wireless Communications and Networking Conference (WCNC)*, 2017.
[15] Qiu, Lanxin, et al. “Multifrequency Phase Difference of Arrival Range Measurement: Principle, Implementation, and Evaluation.” *International Journal of Distributed Sensor Networks*, vol. 11, no. 11, 2015, p. 715307.
[16] “Phase Synchronization Capability of TwinRX Daughterboards and DoA Estimation” https://github.com/EttusResearch/gr-doa/blob/master/docs/whitepaper/doa_whitepaper.pdf
[17] http://www.its.caltech.edu/~matilde/GaborLocalization.pdf
[18] Goldsmith, Andrea. *Wireless Communications*. Cambridge University Press, 2004.
[19] Zekavat, Reza, and Michael Buehrer. *Handbook of Position Location: Theory, Practice and Advances*. IEEE-Wiley, 2012.
[20] Scher, Aaron “How to capture raw IQ data from a RTL-SDR dongle and FM demodulate with MATLAB”
[21] H. K. Hwang, Z. Aliyazicioglu, M. Grice, and A. Yakovlev, “Direction of Arrival Estimation using a Root-MUSIC Algorithm” March, 2008.